Modeling Residual Stresses in Spring Steel Quenching

G. Sánchez Sarmiento[1] , M. Castro[1] , G.E. Totten[2] , L.M. Jarvis[3] , G. Webster[2] and M. F. Cabré[4]

1) Universidad de Buenos Aires, Facultad de Ingeniería, Buenos Aires, Argentina.
2) Dow Chemical Co., Tarrytown, NY, USA.
3) Tenaxol Inc., Milwakee, Wisconsin, USA.
4) Universidad del Salvador, Buenos Aires, Argentina.

Abstract

A comparative study of residual stresses and distortion in cylindrical samples of AISI 5160H spring steel, quenched at different bath temperatures both in 25 % aqueous solutions of Polyalkilene glycol UCON quenchant HT, as well as in Arco 521 oil, is presented in this article. The probe diameters are 0.81 and 0.53 inches.

The ABAQUS/Standard Finite Element Software was applied to assess residual stresses and distortion during the heat treatment, with previous calculations of the heat transfer coefficients as dependent of the temperature by means of the INC-PHATRAN Code. The inverse heat conduction problem coupled with phase transformation is solved by INC-PHATRAN knowing the cooling curves measured by thermocouples placed at the center of each sample.

Valuable conclusions about the use of both quenchants, intended to minimize distortion and cracking problems during heat treating, are the results of the present work.

Introduction

Comparisons of different quenchants in heat treatment processes of steels are of great usefulness in order to control residual stresses, cracking, and distortion of the pieces. The mathematical modeling of these processes is nowadays an indispensable tool for that purpose.

The present work consists of a comparative study of the distorsion and residual stress distribution in cylindrical samples of AISI 5160H spring steel, quenched in 25 % aqueous solutions of Polyalkilene glycol UCON quenchant HT, as well as in Arco 521 oil, at different bath temperatures. The diameters of the probes are 0.81 and 0.53 inches. Cooling curves were measured by thermocouples placed at the center of each probe. Based on these cooling curves, a finite element computer simulation of the processes was carried out applying succesively the softwares INC-PHATRAN and ABAQUS/Standard, briefly described at follows:

INC-PHATRAN (INverse Conduction coupled with PHAse TRANsformation) [1-6] is a program that may be applied to simulate a great variety of heat treatment processes, in planar geometries as well as in axysimmetrical ones, by means of a finite element approach. The corresponding heat transfer coefficients can be calculated with its help, if cooling curves taken from different locations of the heat treated component are provided. The model is based on a numerical optimization algorithm which includes a module responsible for calculating on time and space the temperature distribution and its coupled microstructural evolution. The transformation from austenite to ferrite, perlite and martensite is governed by the appropriate TTT curve and also by the Avrami's approximation. The temperature evolution, as measured by thermocouples at different positions in the component, are used as input for the program. The program calculates the time variation of the heat transfer coefficients, together with the temperature and distribution of phases, and their variation in time throughout the component.

The general purpose finite element system **ABAQUS/Standard** [7] was used to simulate the distortion and the residual stresses produced in the studied samples, as a consequence of a heat treatment process, with previous calculation of the temperature distribution pattern in each case, based on the heat transfer coefficients obtained with INC-PHATRAN.

A series of valuable conclusions about the use of 25 % aqueous solutions of Polyalkilene glycol UCON quenchant HT, as well as in Arco 521 oil and in pure water, intended to minimize distortion and cracking problems during heat treating, have been here obtained.

Measurements of cooling curves

Twelve AISI 5160 steel cylindrical samples of 0.81 and 0.53 inches in diameter were thermically treated in order to study the properties of two different

quenchants. Such samples were manufactured by Moog (St. Louis, MO, USA) and treated by Tenaxol Inc. (Milwaukee, WI, US) using quenchants provided by Union Carbide Co. (Tarrytown, NY, USA). Samples 1 to 6 were quenched in aqueous solution of PAG (Poly Alkylene Glycol) UCON HT with a concentration of 25%, while sample 7 to 12 were quenched in Arco 521 oil. Odd numbered samples was of 0.81 inches in diameter while even numbered samples was of 0.53 inches. The first four columns of Table 1 show the number of each sample, its diameters, the quenchant used and its temperature.

Temperatures were acquired by a thermocouple placed in the center line of each cylinder, which was connected to a computer to carry out the data acquisition process, with a known frecuency. These curves were then kept in numerical files which were afterwards used to feed INC-PHATRAN Code.

Computer Simulations with Program INC-PHATRAN

The simulations performed with INC-PHATRAN Code used a finite element mesh containing 20 nodes along the radial direction and 3 nodes along the longitudinal direction, which is shown in Figure 1. For the discretization of the time variable were chosen 180 time steps. Most of the microstructural transformations occured during the first minute, therefore these were the times taken into account for the simulations.

The total time of each process were divided into a certain quantity of time intervals where the heat transfer coefficient varies linearly. The election of both the initial values for these coefficient and the quantity and lenght of the time intervals depended on each sample. The mean square difference between the measured and calculated temperatures obtained after the optimization of the heat transfer coefficients was about 1 °C. Table 2 shows the heat transfer coefficients obtained for each sample for temperatures between 200 °C and 800 °C.

As an example, the heat transfer coefficient as a function of temperature obtained after mathematical simulation of sample # 11 is shown in Figure 2. The measured and calculated cooling curves for the same sample are plotted in figure 3, whereas figure 4 shows the difference between measured and calculated temperatures as a function of time.

Figures 5 to 8 show the calculated heat transfer coefficients as a function of temperature, comparing the quenching power of the two quenchants studied. UCON 25 % shows a peak in the heat transfer coefficient near 500 °C, whereas the maximum values of this variable for ARCO 521 are in the range of 620 - 780 °C.

Sample #	Quenchant	Diameter		Temperature	
		[inch]	[mm]	[°F]	[°C]
1	UCON 25 %	0.81	20.56	120	48.9
2	UCON 25 %	0.53	13.45	120	48.9
3	UCON 25 %	0.81	20.56	140	60.0
4	UCON 25 %	0.53	13.45	140	60.0
5	UCON 25 %	0.81	20.56	160	71.1
6	UCON 25 %	0.53	13.45	160	71.1
7	ARCO 521	0.81	20.56	120	48.9
8	ARCO 521	0.53	13.45	120	48.9
9	ARCO 521	0.81	20.56	140	60.0
10	ARCO 521	0.53	13.45	140	60.0
11	ARCO 521	0.81	20.56	160	71.1
12	ARCO 521	0.53	13.45	160	71.1

Table 1: Diameter, quenchant, temperature of the quenchant and mean square difference between the measured and calculated temperatures for each one of the treated samples

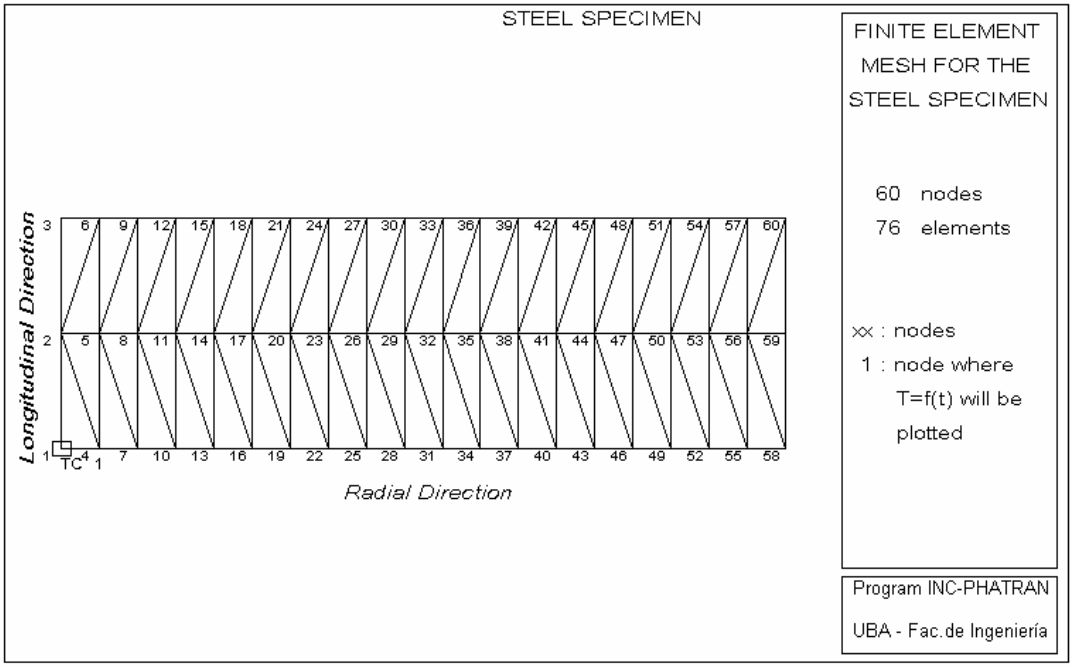

Figure 1: Finite element mesh for each of the treated samples.

Quenchant	Diameter of the probe [mm]	Temperature of the quenchant [°C]	Sample #	Heat Transfer Coefficient [w/m^2°C]						
				200 °C	300 °C	400 °C	500 °C	600 °C	700 °C	800 °C
PAG UCON HT 25 %	20.56	48.9	1	---	---	1500	1350	1350	1800	1100
		60.0	3	---	---	1050	2100	1000	1550	600
		71.1	5	---	1000	1180	1600	900	640	560
	13.45	48.9	2	---	---	1500	1850	1300	1150	700
		60.0	4	---	---	1250	2100	1150	1100	650
		71.1	6	---	760	1180	1530	850	760	480
ARCO 521	20.56	48.9	7	---	900	1100	2000	1700	2950	2150
		60.0	9	400	950	2200	2250	2600	3000	3650
		71.1	11	---	1150	1550	1900	2150	2550	2900
	13.45	48.9	8	---	700	1600	1300	1850	2400	1300
		60.0	10	550	650	1350	1650	1800	1700	1100
		71.1	12	---	550	1200	1950	1800	1600	1500

Table 2: Heat transfer coefficient evolution as dependent of the temperature, calculated by INC-PHATRAN code.

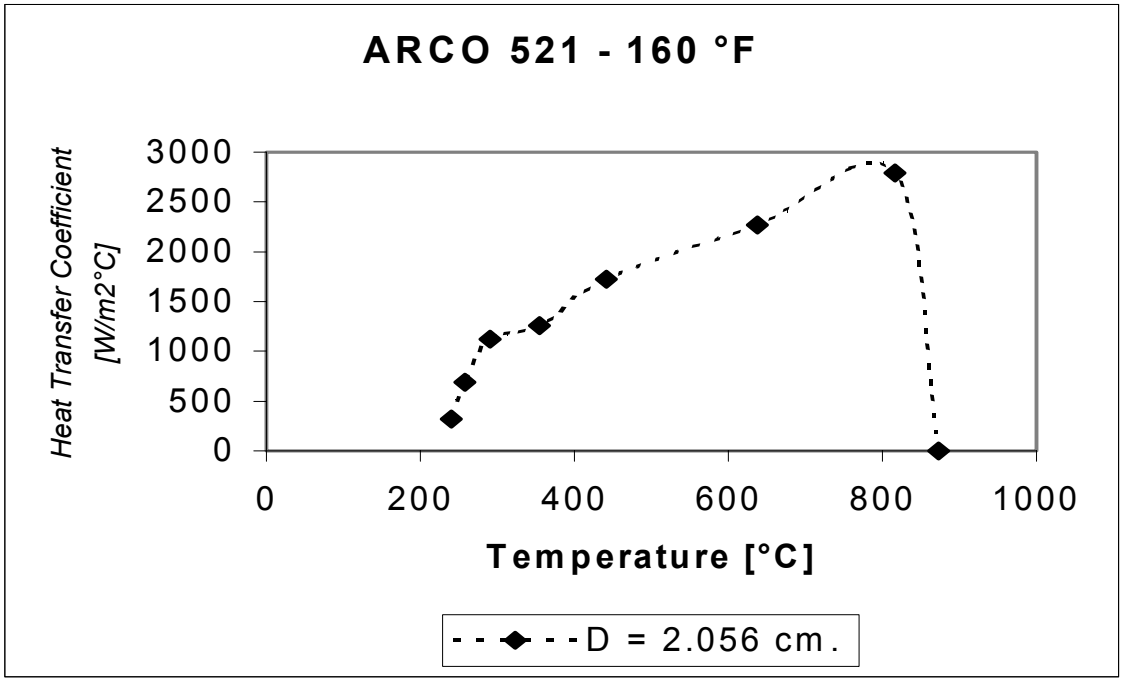

Figure 2: Heat transfer coefficient of Sample # 11.

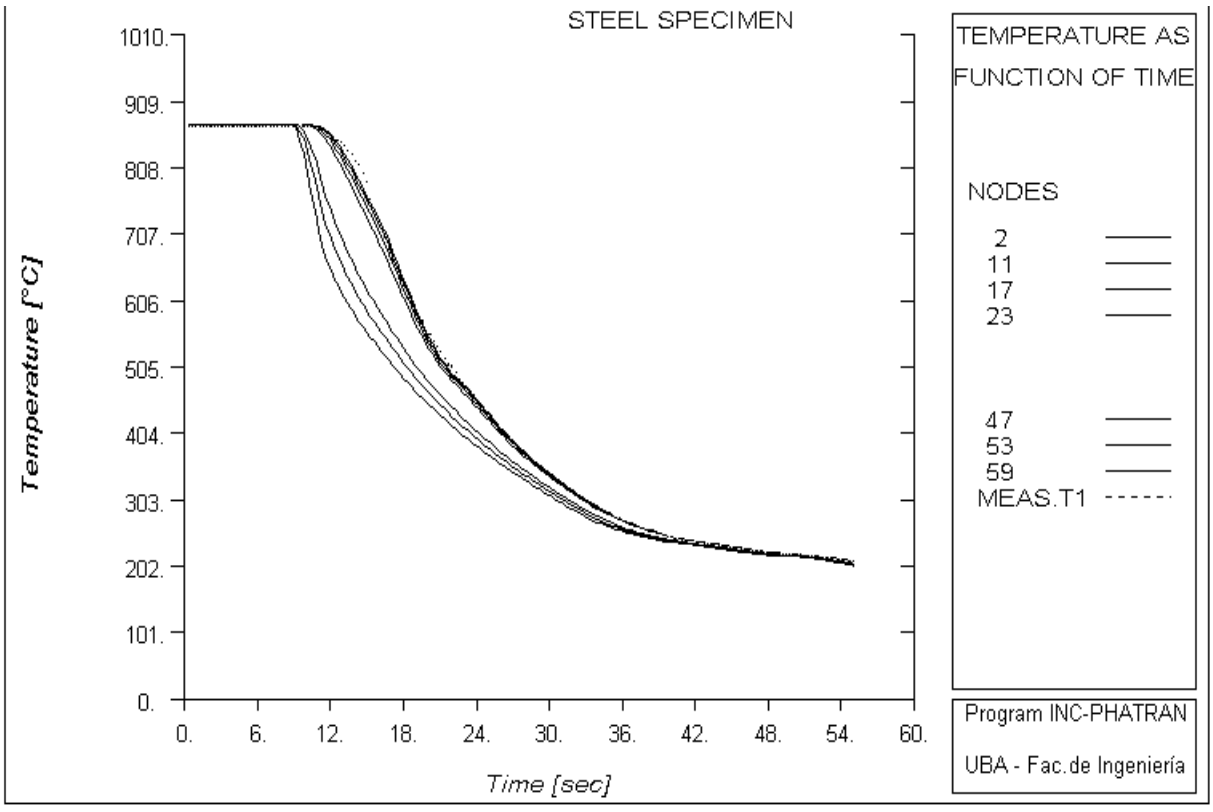

Figure 3: Measured and calculated cooling curves for sample # 11.

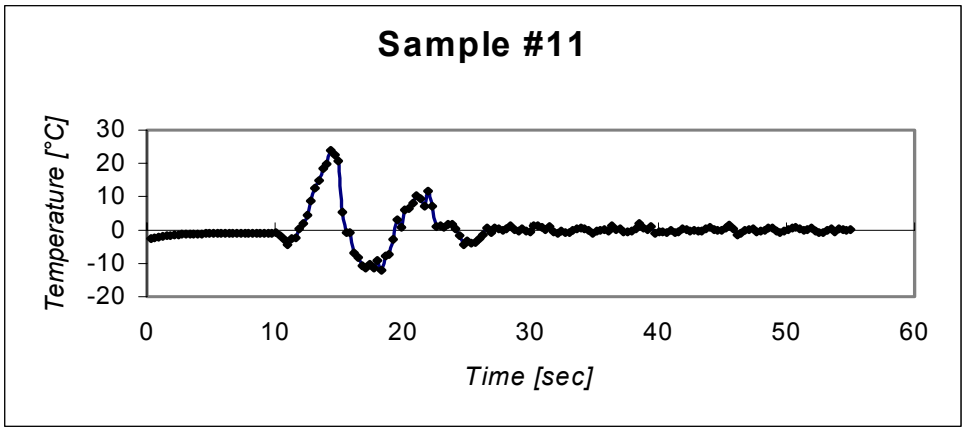

Figure 4: Difference between measured and calculated temperatures for sample #11.

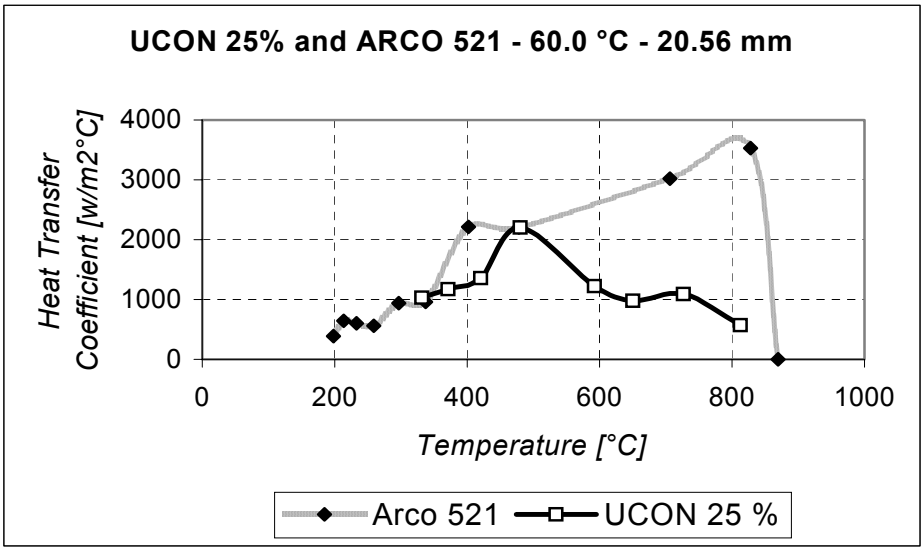

Figure 5: Heat transfer coefficient as function of temperature after mathematical simulation of samples #3 and #9. Quenching media: 25 % UCON HT and Arco 521. Sample diameter: 20.56 mm. – Quenchant temperature: 60.0 C

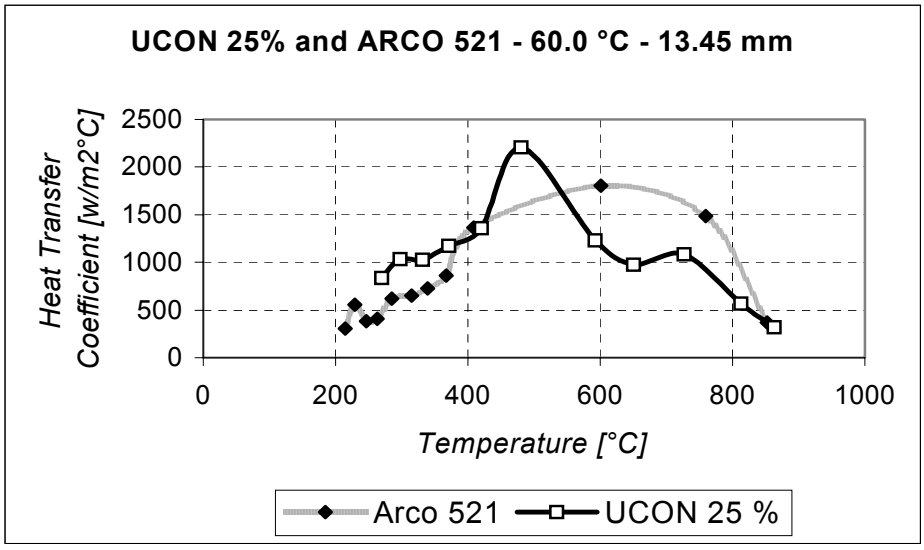

Figure 6: Heat transfer coefficient as function of temperature after mathematical simulation of samples #4 and #10. Quenching media: 25 % UCON HT and Arco 521. Sample diameter: 13.45 mm. – Quenchant temperature: 60.0 °C

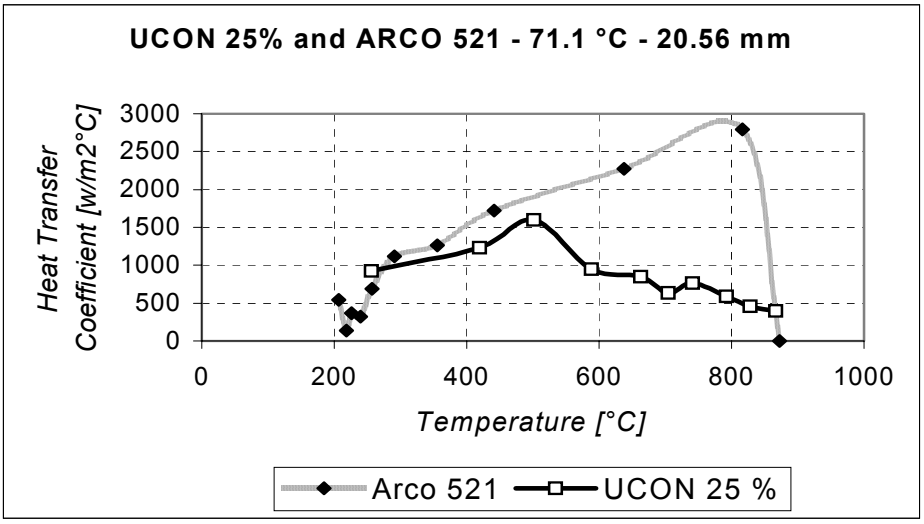

Figure 7: Heat transfer coefficient as function of temperature after mathematical simulation of samples #5 and #11. Quenching media: 25 % UCON HT and Arco 521. Sample diameter: 20.56 mm. – Quenchant temperature: 71.1 °C.

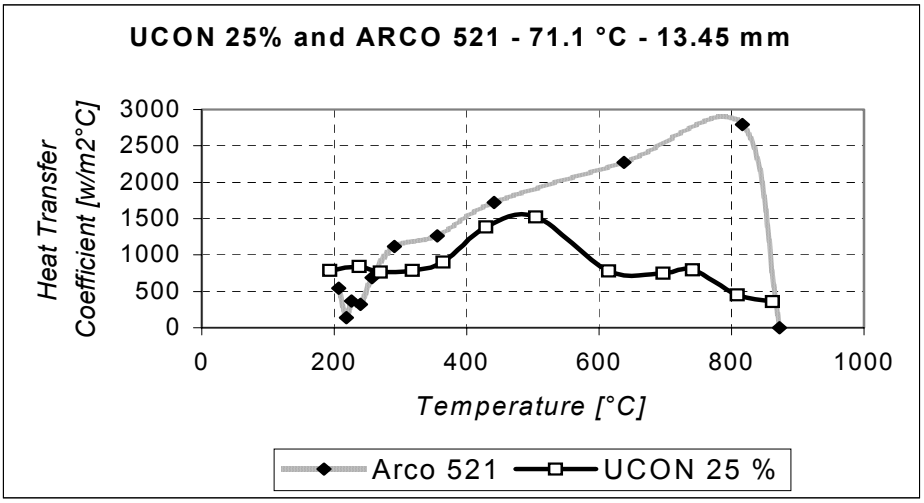

Figure 8: Heat transfer coefficient as function of temperature after mathematical simulation of samples # 6 and # 12. Quenching media: 25 % UCON HT and Arco 521. Sample diameter: 13.45 mm. – Quenchant temperature: 71.1 °C.

Computer simulations with ABAQUS/ Standard

The heat transfer coefficients obtained for the twelve samples described before were used as input for ABAQUS/Standard in order to calculate the thermal field, again as well as the corresponding distribution of thermal stresses depending on time, during the heat treating process. Calculations showed that such stresses were not high enough to generate residual stresses. Figures 9 and 10 show the time evolution of these temperatures and the difference between them, respectively, for sample # 1. The same plots for sample # 11 are shown in figures 11 and 12 respectively.

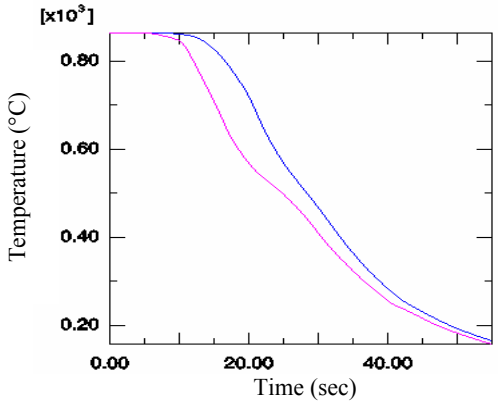

Figure 9: ____ : temperature on the surface of sample #1. ____ : temperature in the center of sample #1.

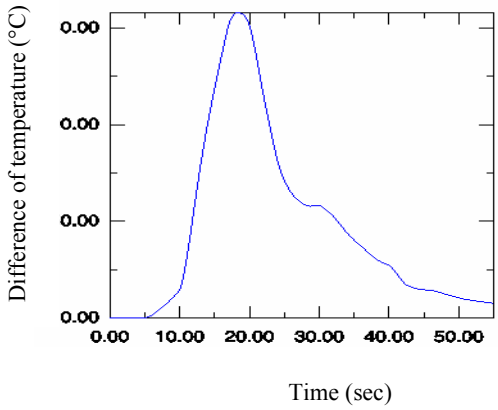

Figure 10: Difference between temperatures in the center and on the surface of sample #1.

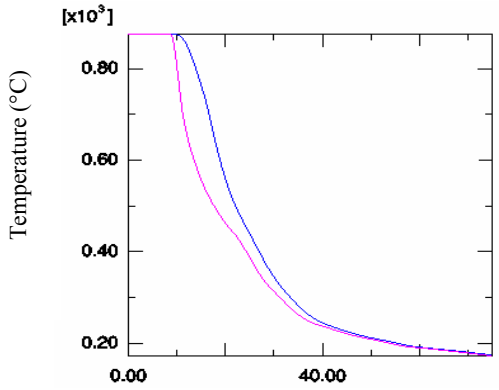

Figure 11: ____ : temperature on tthe surface of sample #11.____ : temperature in the center of sample #11.

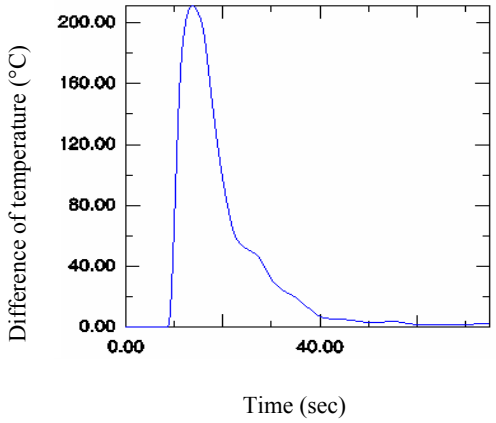

Figure 12: Difference between temperatures in the center and on the surface of sample #11.

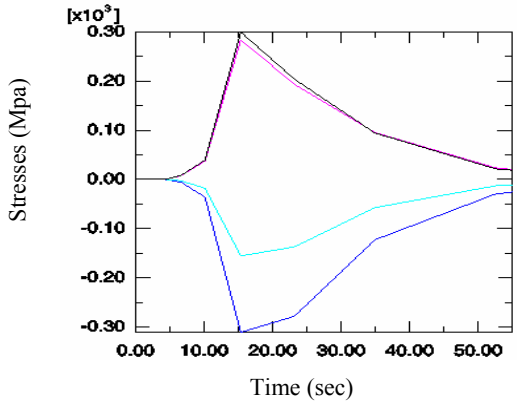

Figure 13: ____ : σ_z in the center ____ : σ_z on the surface ____ : σ_θ in the center ____ : σ_θ on the surface. (Sample #1).

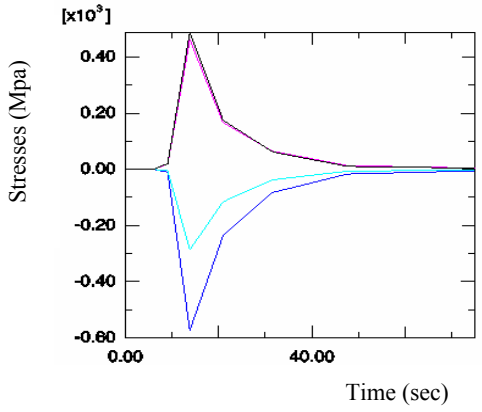

Figure 14: ____ : σ_z in the center ____ : σ_z on the surface ____ : σ_θ in the center ____ : σ_θ on the surface. (Sample #11).

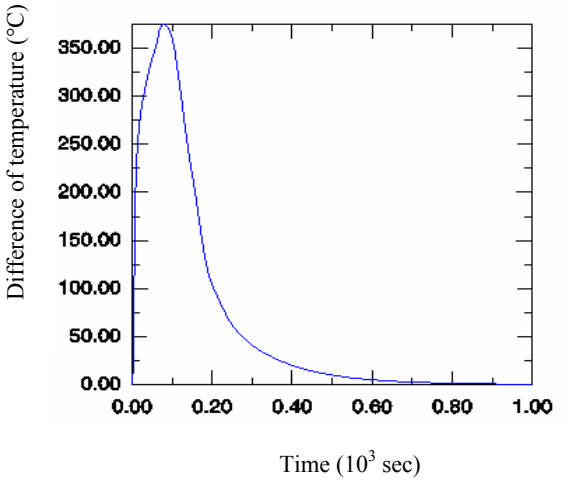

Figure 15: Difference between temperatures in the center and on the surface

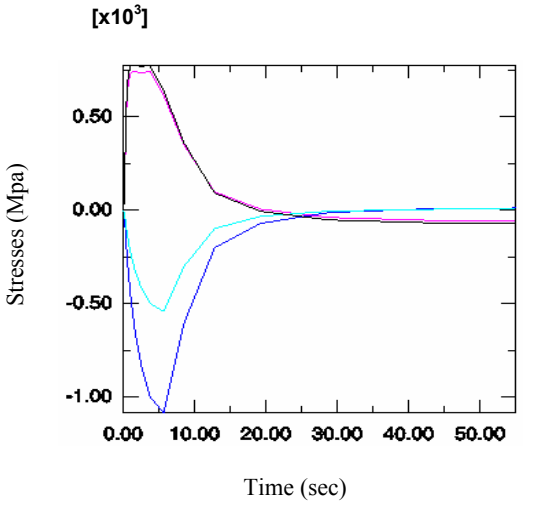

Figure 16: ____ : σ_z in the center ____ : σ_z on the surface ____ : σ_θ in the center ____ : σ_θ on the surface. (Sample #11).

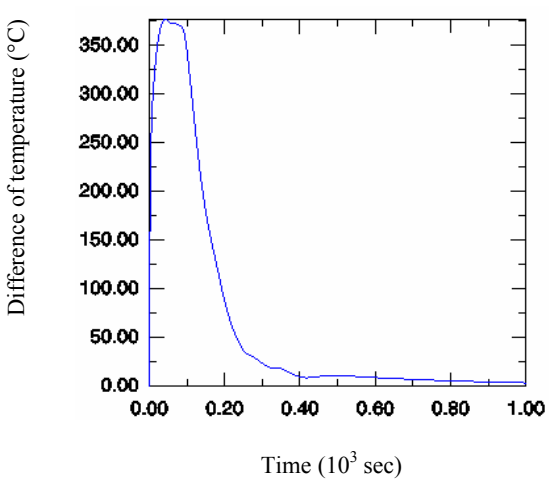

Figure 17: Difference between temperatures in the center and on the surface.

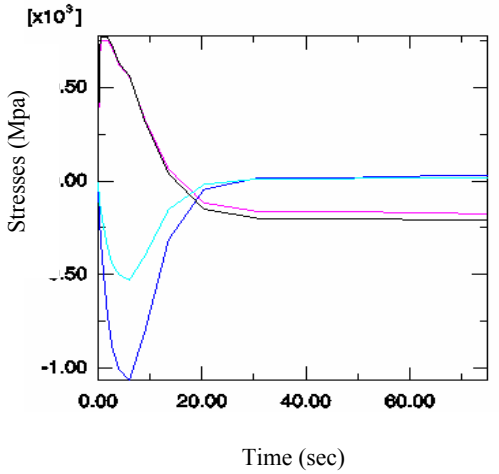

Figure 18: ____ : σ_z in the center ____ : σ_z on the surface ____ : σ_θ in the center ____ : σ_θ on the surface. (Sample #11).

After thermal field are known for each sample, the corresponding thermo-elastic-plastic problem is solved also by ABAQUS/Standard. Figure 13 shows the evolution of the longitudinal and hope stresses at the center and at the surface of sample #1 during the quenching, while Figure 14 shows the same plot but for sample # 11.

In order to analyse the dependance of residual stress on the size of the treated sample, two simulations were developed for bigger steel cylinders, which were of 10 cm in diameter and 20 cm in length. For the first simulation quenchant UCON HT 25 % aqueous solution at 49.9 °C was considered, while for the second one, ARCO 521 at 71.1 °C was the quenchant taken into account. Figure 15 shows the time evolution of the difference between the temperature in the center of the cylinder and the temperature on its surface for the first simulation, which reachs a maximum value greater than 350 °C and is high enough to generate residual stress after the thermal process was carried out, as it can be observed in Figure 16. Figures 17 and 18 show the same plots but for the second simulation. The residual stress calculated in this case is greater than that of the first simulation, in which a polymeric solution was considered.

Finally, a thermal process for a 10 cm diameter and 10 cm length steel cylinder using water, was also simulated. The difference between the temperature in the center of the cylinder and the temperature on its surface reachs a maximum value hardly below 600 °C as it is displayed in Figure 19. The greater this difference of temperature is, the greater the residual stress is obtainned after the process. Figure 20 shows the time evolution of the longitudinal and angular components of the stress in the center of the cylinder and on its surface.

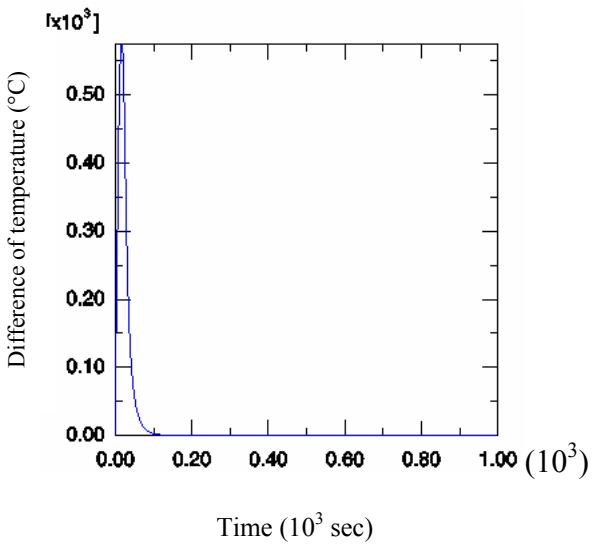

Figure 19: Difference between temperatures in the center and on the surface.

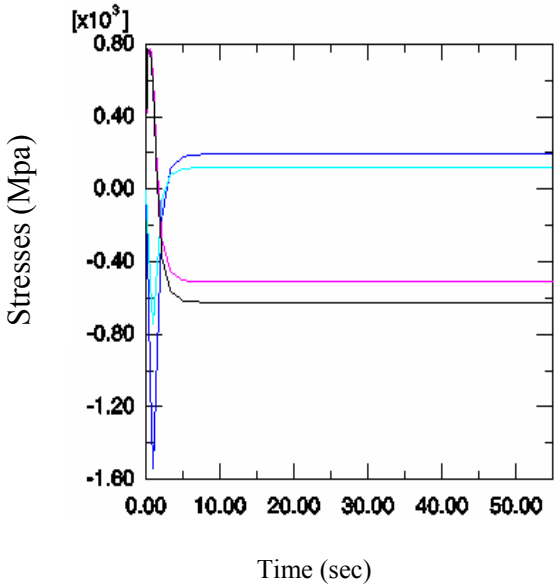

Figure 20: ____ : σ_z in the center ____ : σ_z on the surface ____ : σ_θ in the center ____ : σ_θ on the surface. (Sample #11).

Conclusions

A comparative study of residual stresses and distortion in cylindrical samples of AISI 5160H spring steel quenched in aqueous solutions of Polyalkilene glycol UCON quenchant HT, and in Arco 521 oil, has been presented in this article. Several conclusions may be drawn from these calculations:

1) The heat transfer coefficients obtained for UCON 25 % show a peak varying from 1500 to 2100 w/m^{2}K, at about 500 °C, whereas the maximum values of this variable for ARCO 521 oil are in the range of 1900 – 3500 w/m^{2}K at a temperature interval of 620 - 780 °C.
2) With both quenchants there is no residual stresses after the heat treatment of the cylindrical probes of AISI 5160H spring steel studied, with diameters of 13.45 and 20.56 mm.
3) With PAG UCON quenchant HT, residual stresses would appear for cylindrical pieces of as greater as 10 cm in diameter. On the other hand, cylindrical pieces of the same material and of about 5 cm in diameter quenched in Arco 521 oil may have residual stresses. Cylindrical pieces of 10 cm in diameter quenched in Arco 521 will have residual stresses of about 250 MPa after quenching (for comparison, these stresses reach 640 MPa if the same probe are quenched in water).
4) The combination of INC-PHATRAN and ABAQUS/Standard softwares are very valuable for the determination of residual stresses and distortion in heat treatment of steels pieces having arbitrary geometries.

Acknowledgements.

The authors thank the support given by Universidad de Buenos Aires, Argentina, through the Grant UBACYT TI035 (1998-2000).

References.

1. G. Sánchez Sarmiento y C. Barragán, "INC-PHATRAN: A computer model for the simulation of heat-treating processes, User manual", SOFT-ING Consultores, Abril de 1997.
2. G. Sánchez Sarmiento, C. Barragán y J. Vega: "Predicting hardeness distribution after heat treating processes of steels by finite element simulation combined with the SAE Standard J406". *Milam et al, Eds: HEAT TREATING - Proceedings of the 17th Heat Treat EXPO & Technical Conference,* ASM - Heat Treating Society, Indianapolis, USA, 15 al 18 de septiembre de 1997, pp 347-354.
3. G. Sánchez Sarmiento, A. Gastón y J. Vega: "Inverse heat conduction coupled with phase transformation problems in heat treating process". *E. Oñate and S.R. Idelsohn, Eds.: COMPUTATIONAL MECHANICS - New Trends and Applications.* CIMNE, Barcelona, España, 1998. CD-Book. Part VI, Section 1, Paper 16.

4. G. Sánchez Sarmiento, M.A. Morelli y J. Vega: "Improvements to the SAE J406 Hardenability Predictor". *R. Colás et al, Eds.: Proceedings of the 1st International Automotive Heat Treating Conference*, ASM International, Puerto Vallarta, México, 13 al 15 de julio de 1998, pp 401-414.
5. G. Sánchez Sarmiento, J. Vega, M.A. Morelli, J.C. Cuyás, A.I. Ledesma y M.J.A. Solari: "Predicting hardness of stainless steels in tempering cycles with variable temperature ". *Proceedings of the 19st ASM Heat Treat Expo & Technical Conference,* Cincinnati, OH, Nov. 1-4, 1999.
6. G. Sánchez Sarmiento y J. Vega: "Calculation of the hardness space distribution in the as quenched condition of a medium hardening tool steel". *1st International Conference on Thermal Process Modeling and Computer Simulation*, Shanghai Jiao Tong University, Shanghai, China, 28 al 30 de marzo de 2000.
7. Hibbitt, Karlsson and Sorensen, Inc.: "ABAQUS/Standard. User's Manual". Versión 6.2. 2001.